NACA

RESEARCH MEMORANDUM

PRELIMINARY INVESTIGATION OF A SUPERSONIC SCOOP INLET DERIVED FROM A CONICAL-SPIKE NOSE INLET

By Charles E. Wittliff and Robert W. Byrne

Langley Aeronautical Laboratory
Langley Field, Va.

NATIONAL ADVISORY COMMITTEE FOR AERONAUTICS
WASHINGTON
September 11, 1951

NATIONAL ADVISORY COMMITTEE FOR AERONAUTICS

RESEARCH MEMORANDUM

PRELIMINARY INVESTIGATION OF A SUPERSONIC SCOOP INLET DERIVED FROM A CONICAL-SPIKE NOSE INLET

By Charles E. Wittliff and Robert W. Byrne

SUMMARY

A preliminary investigation has been conducted on a supersonic scoop inlet derived from a conical-spike nose inlet at Mach numbers of 1.3, 1.6, and 1.9. Comparison of the pressure-recovery results of the scoop inlet with results obtained for conical-spike nose inlets shows that the pressure recoveries were in general agreement for the Mach number range extending from 1.3 to 1.9. Results of the investigation show that removal of the boundary layer by means of a sweptback boundary-layer suction slot ahead of the inlet was found to increase the pressure recovery. It was also found that simple elevation (without suction) of the scoop inlet above the surface on which it was mounted increased the pressure recovery by roughly two-thirds of the increase obtained when suction was applied to the same configuration. When the mass flow through the suction slot was equal to 10 percent of the mass flow through the inlet with a slot height of 0.058 cowling-lip diameter, pressure recoveries for Mach numbers of 1.3, 1.6, and 1.9 were 0.93, 0.94, and 0.89, respectively, for the 25° half-cone scoop inlet. For this condition, also, the pressure recovery was found to be approximately constant with varying inlet mass flows.

INTRODUCTION

The need of placing radar, armament, or other equipment in the nose of supersonic interceptor aircraft and the desire to eliminate long air ducts, which would occupy a large volume in an already crowded fuselage, have been the chief factors in considering scoop-type inlets. Thus, the need arises for supersonic inlets suitable for installation on the fuselage. One such inlet has been tested at the Gas Dynamics Branch of the Langley Aeronautical Laboratory.

The present inlet consists of a semicircular cowling and a semicone central body. It is similar to the inlet reported in reference 1 cut along a diametral plane. When an inlet is located on the fuselage instead of in the nose of the airplane, the problem of boundary-layer influence arises. If low-energy boundary-layer air were taken into the inlet, it has been shown in subsonic research that a large loss in pressure recovery would occur. Therefore, provision for boundary-layer removal by means of a sweptback suction slot was made on this inlet.

The purpose of the present research was to obtain a preliminary determination of the pressure-recovery characteristics of this scoop inlet at various Mach numbers and to evaluate the influence of boundary-layer removal on the pressure recovery. The test Reynolds number was also varied over a small range to investigate its effect on the pressure recovery. The model was designed so that the height of the boundary-layer suction slot could be varied, in addition to varying the amount of suction applied to the slot. The variation of pressure recovery with entering mass flow was also determined.

SYMBOLS

R	Reynolds number
M	Mach number
p_o	stagnation pressure of free stream
p_f	stagnation pressure after diffusion
ρ	density
V	velocity
A	area
r,θ	polar coordinates
θ_l	cowling-position parameter (angle between axis of diffuser and line joining apex of cone to lip of cowling)
r_1	inside radius of cowling at location of rake
d	diameter of cowling at lip

h	height of top of boundary-layer suction slot
δ	boundary-layer thickness for $\frac{u}{u_o} = 0.99$
δ^*	boundary-layer displacement thickness
m_r	ratio of mass flow through boundary-layer suction slot to mass flow through inlet
m/m_o	ratio of mass flow through inlet to mass flow in a free-stream tube having a cross-sectional area of $\pi d^2/8$
ΔC_D	pressure-drag coefficient of front face of upper lip of boundary-layer slot
u/u_o	ratio of local velocity to free-stream velocity

TEST EQUIPMENT AND METHODS

Test Conditions

The tests were made in an intermittent-blow-down jet supplied with low-humidity air from a large pressurized tank. A sketch of the model mounted in the test-section floor is shown in figure 1. The test-section dimensions were approximately 4 by $4\frac{1}{4}$ inches. Three sets of wooden nozzle blocks were used to produce the various test Mach numbers. A total-pressure and static-pressure rake was used to calibrate the nozzles. The pressure readings were recorded photographically from pressure gages and U-tube manometers. The Reynolds number for the tests was varied by changing the stagnation pressure. The tests at $M = 1.3$ were run at Reynolds numbers, based on cowling-lip diameter, of approximately 2.5×10^6, 3.8×10^6, and 4.5×10^6. At $M = 1.6$, the Reynolds numbers were 2.7×10^6, 4.0×10^6, and 5.7×10^6. At $M = 1.9$ the test Reynolds numbers were 2.1×10^6, 3.6×10^6, and 5.1×10^6. All tests were made at zero angle of attack, since the model was mounted on the floor of the test section.

Models

The scoop-inlet models tested were two conical-spike nose inlets cut along a diametral plane, as shown in figure 2. One of the inlets had a 25° half-angle conical central body with a 7°, 10° circular cowling.

The other inlet had a 30° half-angle conical central body with a 14°, 17° circular cowling. The angles designating the cowlings refer, respectively, to the inclination of the internal and external sides of the cowling lip with the cowling center line. Both cowlings had a cowling-lip diameter of 1.60 inches. The cylindrical portion of the cowlings had an outside diameter of 2.00 inches and an inside diameter of 1.70 inches. Thus, the cowlings differed only in the vicinity of the lip and were similar to those described in reference 2.

The area ratios of the subsonic-diffuser sections of the inlets are shown in figure 3. The area ratio is referred to the cowling-lip area $\left(A_o = \frac{\pi d^2}{8}\right)$, and the distance is given in cowling-lip diameters from the apex of the central body.

The models were of fixed geometry and the cowling-position parameter θ_l was constant; θ_l was equal to 42.5° for the 25° cone inlet and 48° for the 30° cone inlet. These values corresponded to the shock-wave angles of both cones at a Mach number of 2.0. Thus, when these inlets were tested at $M = 1.9$, the shock waves were slightly ahead of the lip of the cowling for the maximum mass-flow condition.

The boundary-layer suction slot on each model was swept back at an angle equal to the cowling-position parameter θ_l. This value placed the slot at, or behind, the conical shock wave for all test Mach numbers. Because such a design was considered more suitable for practical application than an unswept leading-edge slot, only the sweptback configuration was tested. Having the leading edge of the slot along or behind the conical shock wave reduces the effect of the slot on the flow outside the boundary layer ahead of the inlet. It is theoretically possible to design an unswept slot that would remove the correct amount of boundary layer without creating a disturbance in the flow outside the boundary layer; however, in actual practice, where varying boundary-layer mass flows will be encountered, this design would probably become extremely difficult. These difficulties are alleviated by sweeping back the leading edge of the suction slot. Furthermore, any disturbance created by an unswept slot ahead of the conical shock wave will produce a greater drag than a disturbance by a sweptback slot behind the conical shock wave because the sweptback slot will, if designed similar to the slot reported herein, have a subsonic leading edge. Even if the sweptback suction slot is not designed to remove the entire boundary layer, it will divert most of the portion not removed around the inlet. Unpublished results of an experimental comparison of the swept and unswept leading-edge suction slots in combination with a similar inlet made by the Lewis Laboratory later confirmed these considerations. A cross section of the slot is shown in figure 4.

Measurements

The pressure recovery was measured by three radially placed total-pressure rakes located approximately $4\frac{1}{2}$ cowling-lip diameters from the apex of the central body, as shown in figure 1. There were 11 total-pressure tubes in the rakes. Three static-pressure orifices were also located inside the cowling. A cross section of the inlet showing the location of the total-pressure rakes and the static-pressure orifices is given in figure 5. In reducing the pressure-recovery data, it was assumed that: (1) the flow was symmetrical about the vertical plane; (2) the static pressure was constant throughout the flow in the region of the rakes; and (3) the total-pressure recoveries at each rake were average values for the sector measured by the rake. The symmetry of the model was the justification for the first assumption. Readings obtained from the three static-pressure orifices, located in the vicinity of the rakes, showed that the static-pressure variation was less than 3 percent. In the extreme case, this error resulted in an error of about 5 percent in the value of the local mass flow used for weighting the pressure recovery. Since this value of mass flow so obtained was used only for weighting purposes, its use is believed justified.

The local-pressure recoveries were weighted with respect to mass flow in order to obtain a mean-pressure recovery for the inlet. The mean-pressure recovery was defined as

$$\frac{\bar{p}_f}{p_o} = \frac{\int \frac{p_f}{p_o} \rho V \, dA}{\int \rho V \, dA}$$

For the actual calculations, the cross-section area at the rakes was divided into finite sectors as shown in figure 5. The mean-pressure recovery becomes

$$\frac{\bar{p}_f}{p_o} = \frac{\sum_{\theta} \left(\int_0^{r_1} \frac{p_f}{p_o} \rho V r \, dr \right) \Delta\theta_i}{\sum_{\theta} \left(\int_0^{r_1} \rho V r \, dr \right) \Delta\theta_i}$$

$$(i = 1, 2, 3, 4, 5)$$

The mass flow through the inlet was measured with a calibrated thin-plate orifice contained in a pipe attached to the rear of the model.

Downstream of this orifice was a throttle valve, which was used to regulate the amount of mass flow through the inlet by increasing the back pressure. Shadowgraphs were taken for all test conditions as a check on the amount of throttling and on the mass-flow measurements.

The range of inlet mass flows for which pressure recoveries were measured was limited by aerodynamic considerations. The maximum mass-flow condition was the flow condition obtained just before the inlet shock configuration changed as the mass flow was decreased. The minimum mass flow was determined by the occurrence of aerodynamic instability or, for the case of the $M = 1.3$ tests, until the drag, indicated by the large forward movement of the shock wave as the mass flow was decreased, was considered to be excessive. At Mach numbers of 1.6 and 1.9 the normal shock wave ahead of the cowling lip moves upstream as the mass flow is decreased. When the normal shock has moved a sufficient distance upstream, aerodynamic instability or "buzz" results as described in reference 3. For these Mach numbers the mass flow was decreased until buzz occurred; then the mass flow was increased slightly until the flow was stable.

With this testing technique it was found that the pressure-recovery values could be repeated to within 2 to 3 percent. This variation was due to variations in the amount the mass flow was increased to move slightly away from the buzz condition. At Mach number 1.3, a detached shock wave exists. As the mass flow is reduced, the shock moves upstream with little change in pressure recovery. The upstream movement of the shock wave is associated with an increasing external drag; therefore, pressure-recovery measurements were made only over a small range of mass flows.

The boundary-layer suction-slot height was varied by elevating the upper slot lip, central body, and cowling as a unit. For each setting of the slot height, tests were made with various amounts of suction. A venturi meter having a contraction ratio of 0.5609 was used to measure the mass flow through the boundary-layer slot. Total-pressure and static-pressure measurements indicated that the maximum Mach number in the venturi meter was 0.23; therefore, incompressible-flow equations were used in reducing these mass-flow data. With the inlet elevated above the test-section floor, two configurations without suction were tested: (1) the boundary-layer suction slot was filled in flush with the test-section floor; (2) the slot was open ahead of the inlet, but a valve downstream of the venturi meter was closed.

Total-pressure measurements were made in the boundary layer 1/8 inch ahead of the inlet position with the model removed from the jet. All profiles had turbulent-boundary-layer characteristics. The results of these measurements are given below:

M	R	$\left(\frac{\delta}{d}\right)_{\frac{u}{u_o}=0.99}$	$\frac{\delta^*}{\delta}$
1.9	5.1×10^6	0.136	0.0742
1.6	5.6×10^6	.139	.0712
1.3	4.4×10^6	.0974	.109

These measured values of $\left(\frac{\delta}{d}\right)_{\frac{u}{u_o}=0.99}$ correspond approximately to a boundary layer of 2.5 inches total thickness ahead of an inlet with an 18-inch cowling-lip diameter at $M = 1.9$ and at the same Reynolds number.

Static-pressure measurements were made on the front face of the upper lip of the boundary-layer suction slot in order to determine its pressure drag at a Mach number of 1.9. These measurements were made with the inlet in two elevated positions ($h = 0.025d$, $0.058d$). For these two elevated positions the boundary-layer slot was closed flush with the test-section floor. The pressure measurements were made for the minimum mass-flow condition since this condition corresponded to the greatest drag.

RESULTS AND DISCUSSION

The values of the pressure recovery obtained for various heights of the boundary-layer slot h/d are shown in figures 6(a) and 6(b) for the 25° and 30° cone configurations, respectively. The results presented are for the case of no flow through the boundary-layer-bleed slot both with the slot open and with the slot sealed off flush with the surface of the test section. The values of m/m_o given on the figure are nominal values. The plus and minus values given are variations from these nominal values obtained in the tests made at the different h/d values. It can be seen that the pressure recovery increases continually with increasing slot height for the range of slot heights over which these tests were run. The highest h/d value was well below the measured values of δ/d which were given previously in the section on Tests and Methods.

Comparison of the results of the 25° and 30° cone configurations (fig. 6) shows essentially the same pressure-recovery results for the range of values of h/d over which the models were tested. At a Mach number of 1.9 there is a small increase in pressure recovery with Reynolds number. This increase is probably primarily due to variations of boundary-layer thickness with Reynolds number. Since the changes in pressure recovery with Reynolds number were of the same order as the experimental error, no definite conclusions could be made as to the exact nature of the Reynolds number effects in this preliminary investigation.

In most cases there were only negligible differences in the pressure recovery obtained with the boundary-layer-bleed slot open and with it sealed off flush with the surface of the flat plate (fig. 6).

The pressure drag of the front face of the upper lip of the bleed slot was obtained at a Mach number of 1.9 for values of h/d equal to 0.058 and 0.025 by integrating the static pressures which were measured on the front face of the boundary-layer slot. The static pressures were found to be very close to calculated values of the static pressure behind the conical shock. Drag coefficients based on the inlet lip frontal area were found to be at $M = 1.9$ as follows for the condition of minimum mass flow and the boundary-layer slot closed flush with the surface of the test section:

h/d	ΔC_D
0.058	0.028
.025	.011

The values of drag coefficient represent only the fore drag of the projection of the boundary-layer suction slot.

The results of the tests made with varying amounts of boundary-layer suction at fixed values of h/d are shown for the two cone configurations in figures 7(a) and 7(b). The values of h/d for which the results are presented lie within the measured boundary-layer thickness. It can be seen from figure 7 that most of the improvement in maximum pressure recovery due to suction was obtained in the range of values of m_r between 0 and 0.10 (m_r is the ratio of mass flow through the suction slot to the mass flow through the inlet). As would be expected from the results presented in figure 6, the differences in the boundary-layer-suction results for the two cone configurations are small. Typical shadowgraph pictures of the 25° cone configuration for the minimum mass-flow condition are shown in figure 8.

Figures 9 and 10 present the variation of pressure recovery with mass flow for the 25° cone configuration at h/d values of 0.058 and 0.034, respectively. The variations shown for the h/d value of 0.058 are similar to those shown for the conical spike-nose inlet in that the pressure-recovery values vary little with mass flow. The results for the lower value of h/d (0.034), however, show that the boundary layer passing over the top of suction slot had an appreciable effect on the variation of pressure recovery with mass flow. This effect was also evident in the shadowgraphs which showed for 0.034 h/d that the conical shock was not attached to the cone for low values of m_r but stood slightly ahead of the cone apex.

Figures 11(a) and 11(b) present a comparison of the results of the scoop inlet for the condition of $\frac{h}{d} = 0$, $m_r = 0$ with the results obtained for the condition of $\frac{h}{d} = 0.058$ and m_r values of 0 and 0.10. It can be seen that for this condition approximately two-thirds of the over-all gain obtained by elevating the inlet and applying suction is obtained by merely elevating the inlet.

Also shown in figure 11 is a comparison of the pressure-recovery values obtained in this investigation with the pressure-recovery results obtained with the conical-nose inlets given in reference 1. The figure shows that for a value of $m_r = 0.10$ and $\frac{h}{d} = 0.058$, the results of both cone configurations are in general agreement with the conical-nose-inlet results. No strict comparison can be made between the scoop and nose-inlet results because of the differences in geometry (fig. 11). However, the failure of the scoop-inlet pressure recovery to increase more rapidly than shown with decreasing Mach number between 1.6 and 1.3 is believed characteristic of the operation of a scoop inlet of this type. At a Mach number of 1.3 and at all values of m_r and h/d, for which the tests were run, shadowgraph pictures showed a marked interaction between the conical shock and the boundary layer in which the nose shock was found to stand ahead of the cone apex.

CONCLUSIONS

A preliminary investigation has been conducted on a supersonic scoop inlet derived from a conical-spike nose inlet at Mach numbers of 1.3, 1.6, and 1.9. Comparison of the pressure-recovery results of the scoop inlet with results obtained for conical-spike nose inlets shows that the pressure recoveries were in general agreement for the Mach number range extending from 1.3 to 1.9. Results of the investigation show that removal of the boundary layer by means of a sweptback boundary-layer suction slot ahead of the inlet was found to increase the pressure recovery. It was also found that simple elevation (without suction) of the scoop inlet above the surface on which it was mounted increased the pressure recovery by roughly two-thirds of the increase obtained when suction was applied to the same configuration. When the mass flow through the suction slot was equal to 10 percent of the mass flow through the inlet with a slot height of 0.058 cowling-lip diameter, pressure recoveries for Mach numbers of 1.3, 1.6, and 1.9 were 0.93, 0.94, and 0.89, respectively, for the 25° half-cone scoop inlet. For this condition, also, the pressure recovery was found to be approximately constant with varying inlet mass flows.

Langley Aeronautical Laboratory
National Advisory Committee for Aeronautics
Langley Field, Va.

REFERENCES

1. Ferri, Antonio, and Nucci, Louis M.: Preliminary Investigation of a New Type of Supersonic Inlet. NACA TN 2286, 1951.

2. Ferri, Antonio, and Nucci, Louis M.: Theoretical and Experimental Analysis of Low Drag Supersonic Inlets Having a Circular Cross Section and a Central Body at Mach Numbers of 3.30, 2.75, and 2.45. NACA RM L8H13, 1948.

3. Ferri, Antonio, and Nucci, Louis M.: The Origin of Aerodynamic Instability of Supersonic Inlets at Subcritical Conditions. NACA RM L50K30, 1951.

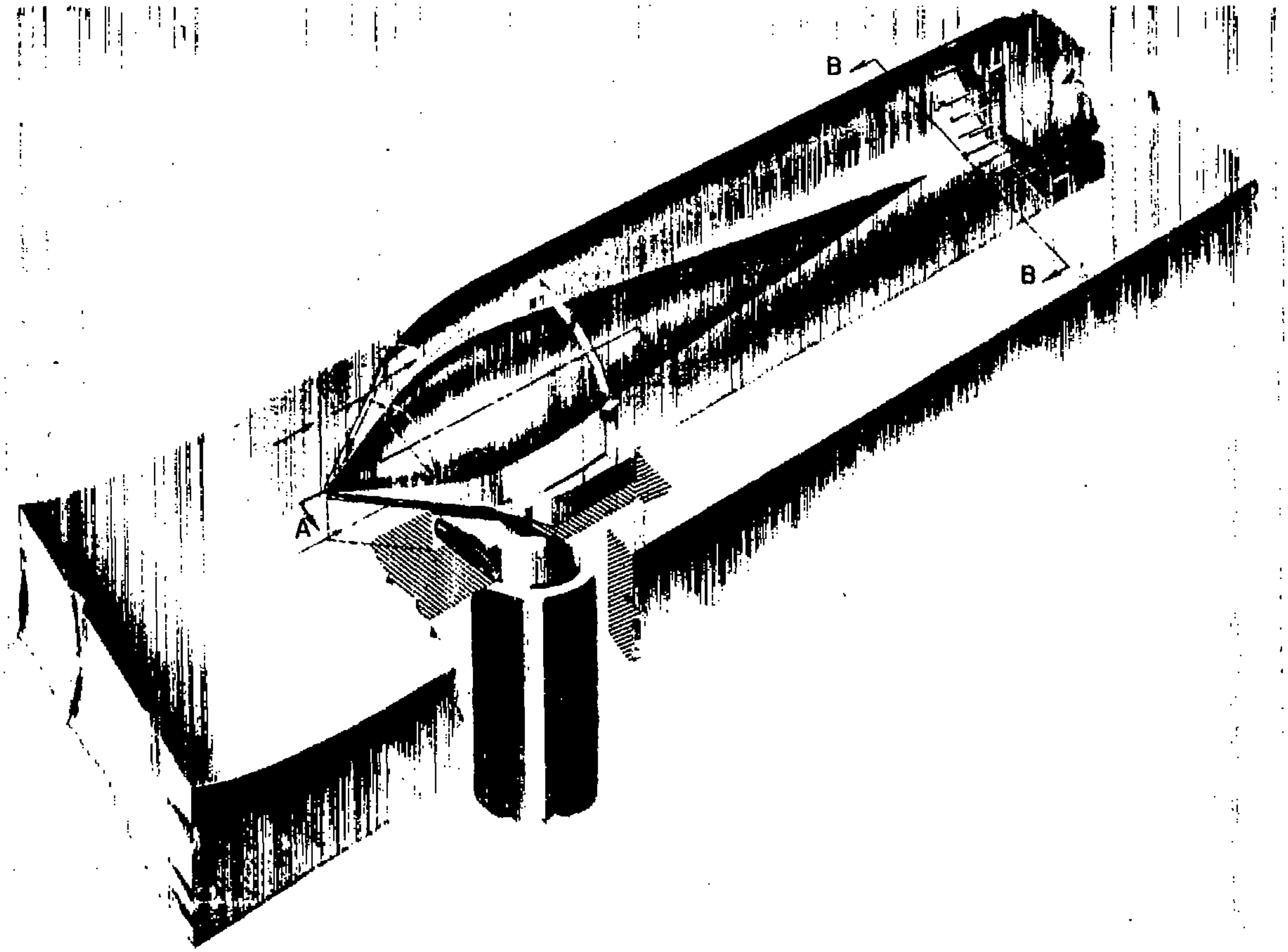

Figure 1.- Schematic drawing of the model mounted in the test-section floor.

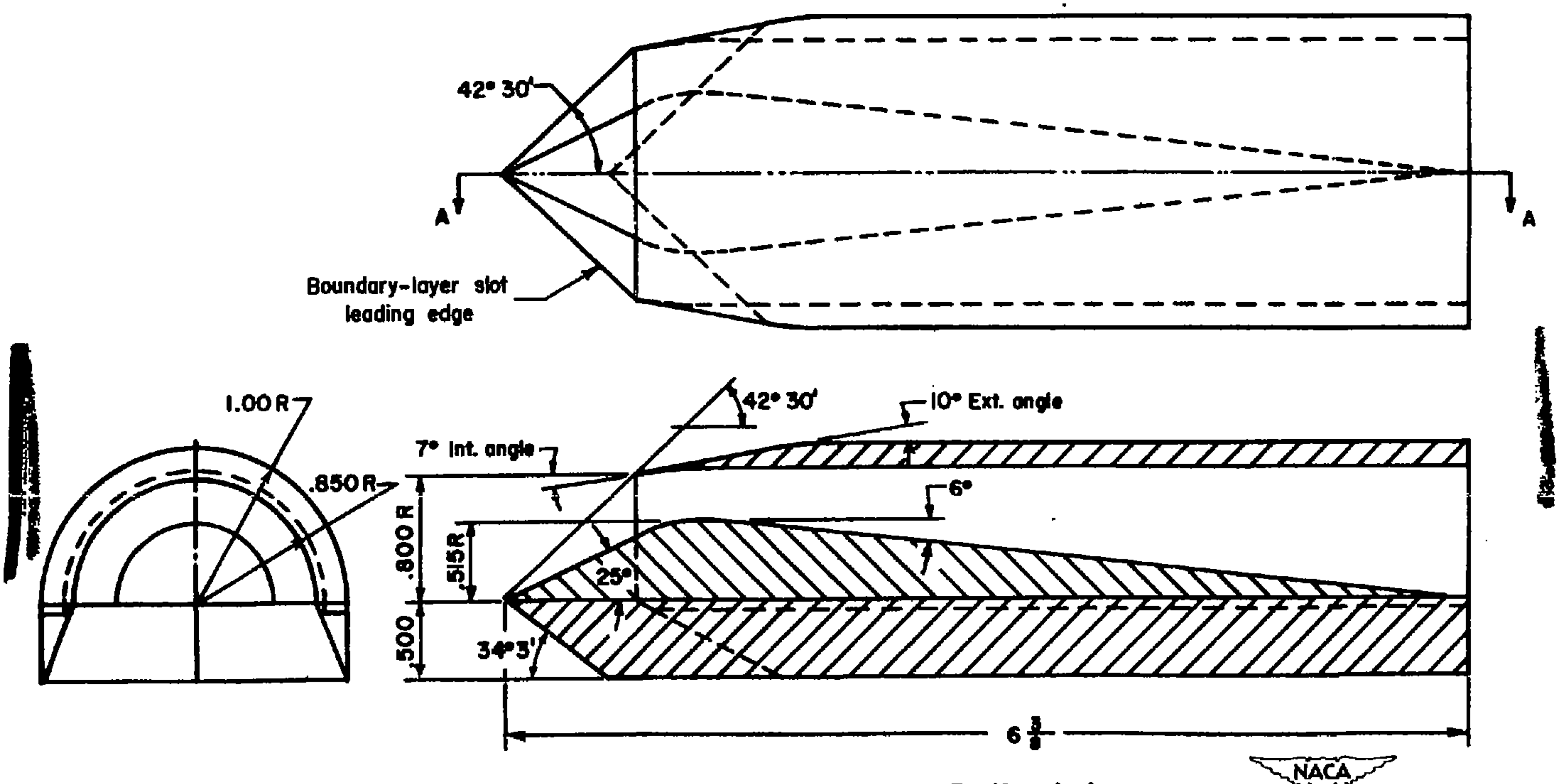

Section A-A

(a) 25° semicone; 7°, 10° cowling.

Figure 2.- Geometry of inlet.

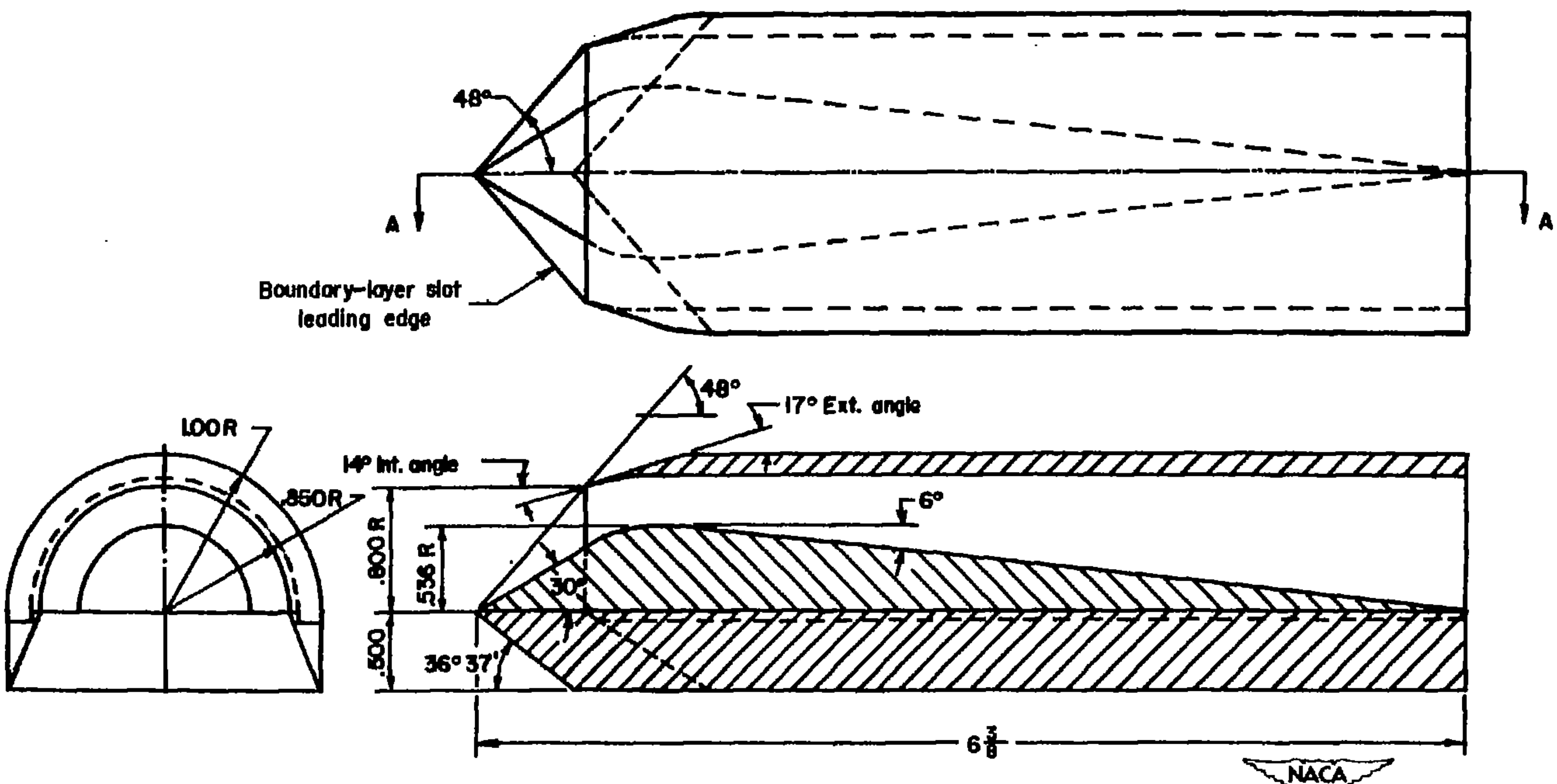

Section A-A

(b) 30° semicone; 14°, 17° cowling.

Figure 2.- Concluded.

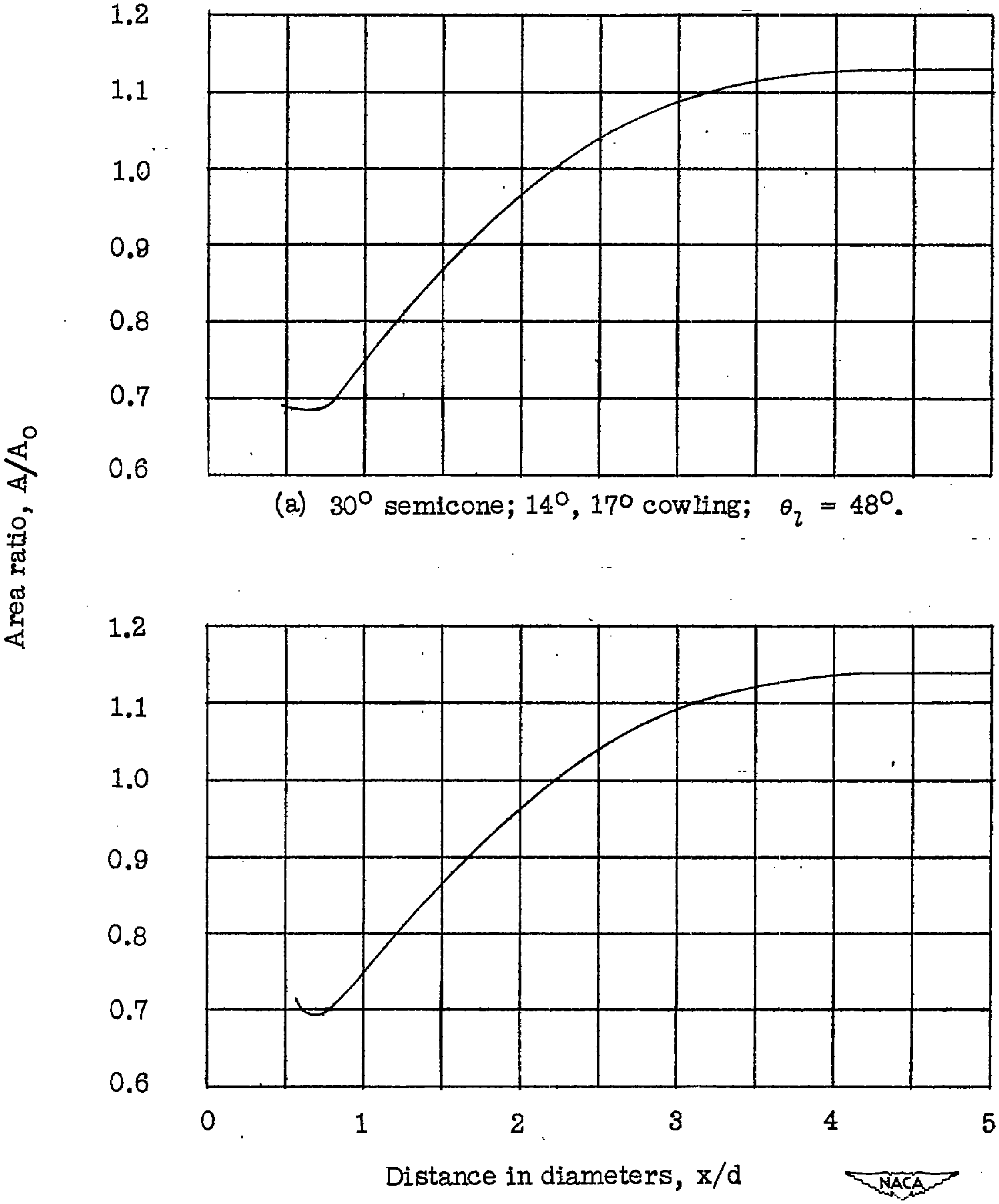

(a) 30° semicone; 14°, 17° cowling; $\theta_l = 48°$.

(b) 25° semicone; 7°, 10° cowling; $\theta_l = 42.5°$

Figure 3.- Area ratio of the inlet as a function of the distance along the axis in cowling-lip diameters.

[redacted]

[redacted]

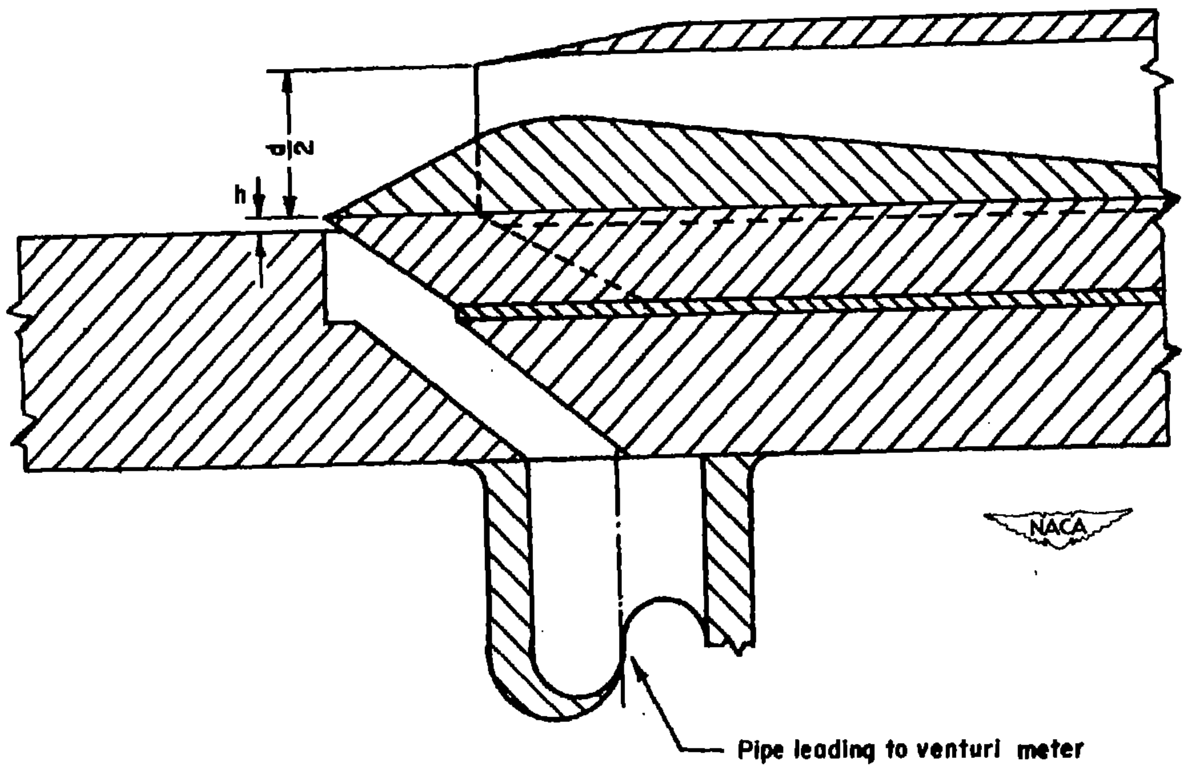

Figure 4.- Section A-A showing boundary-layer suction slot.

[redacted]

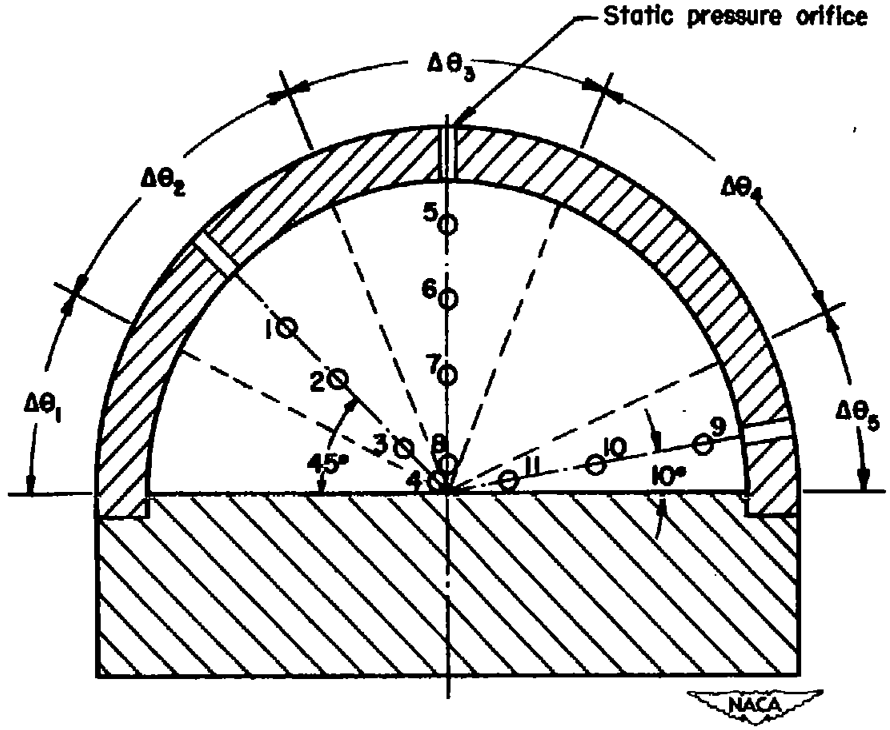

Figure 5.- Section B-B showing position of total-pressure probes in rakes and manner in which the area was subdivided for data reduction.

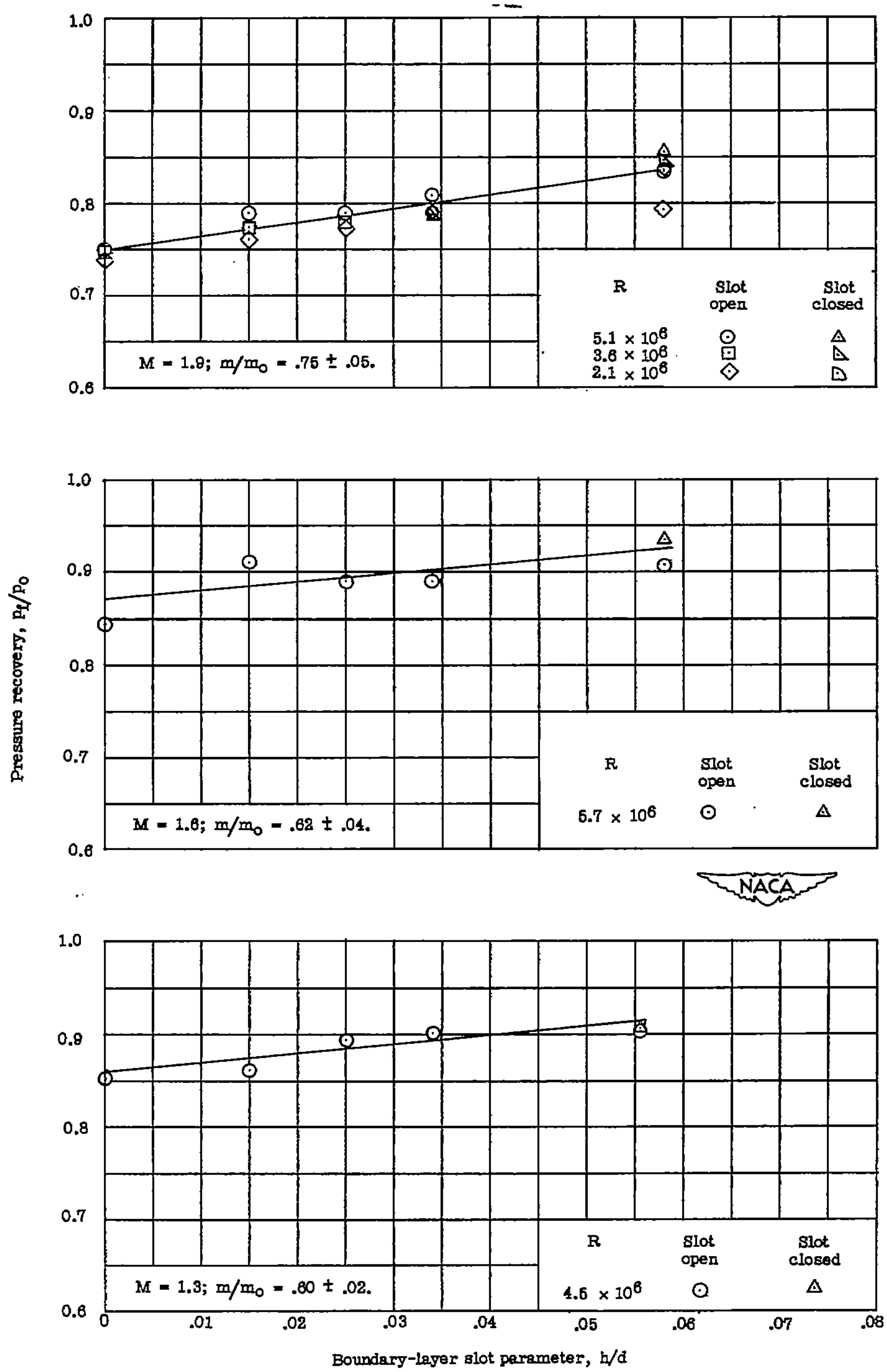

(a) 25° half-cone scoop inlet.

Figure 6.- Pressure recovery as a function of the boundary-layer slot parameter for $m_r = 0$ and minimum m/m_o.

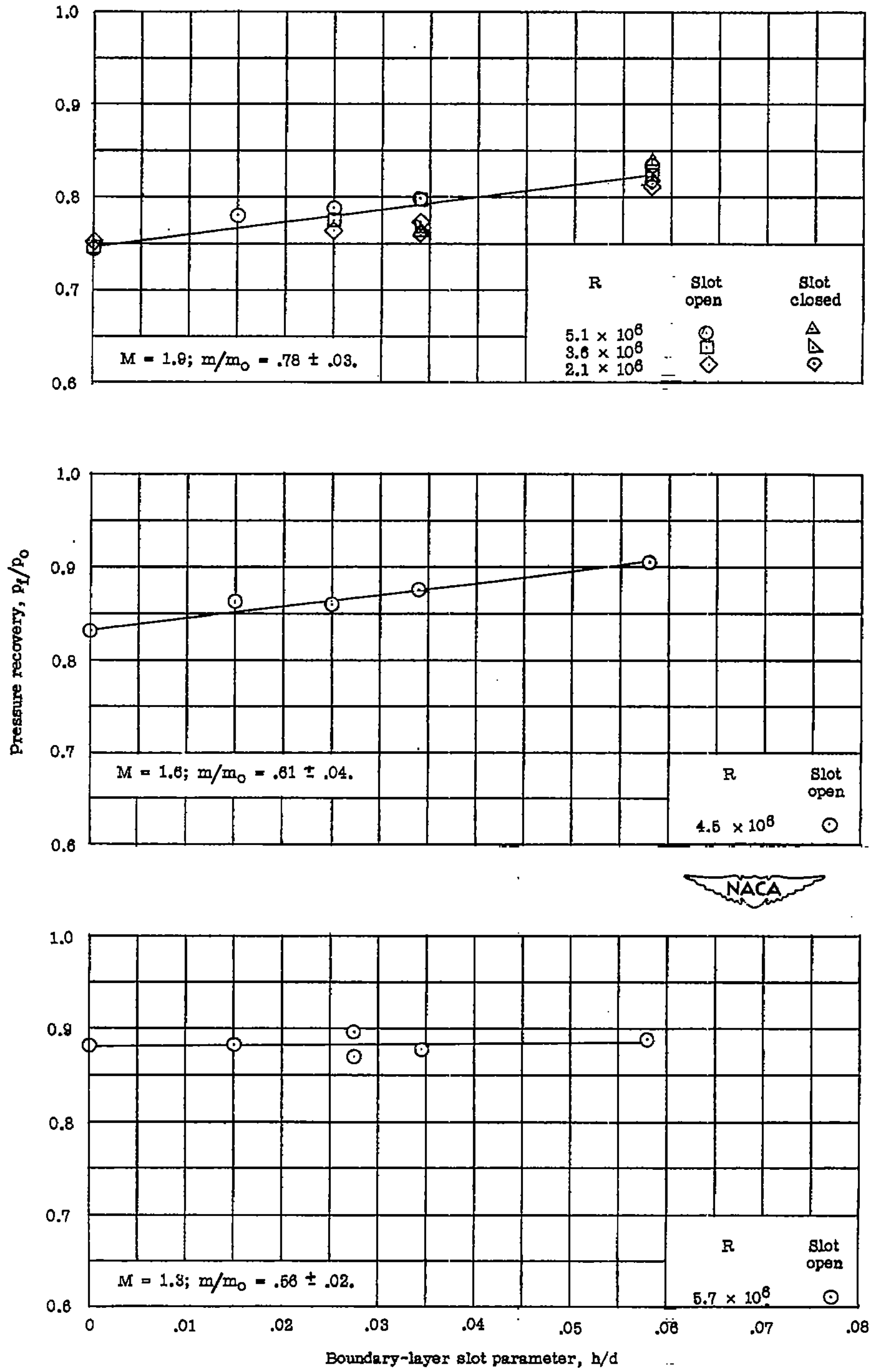

(b) 30° half-cone scoop inlet.

Figure 6.- Concluded.

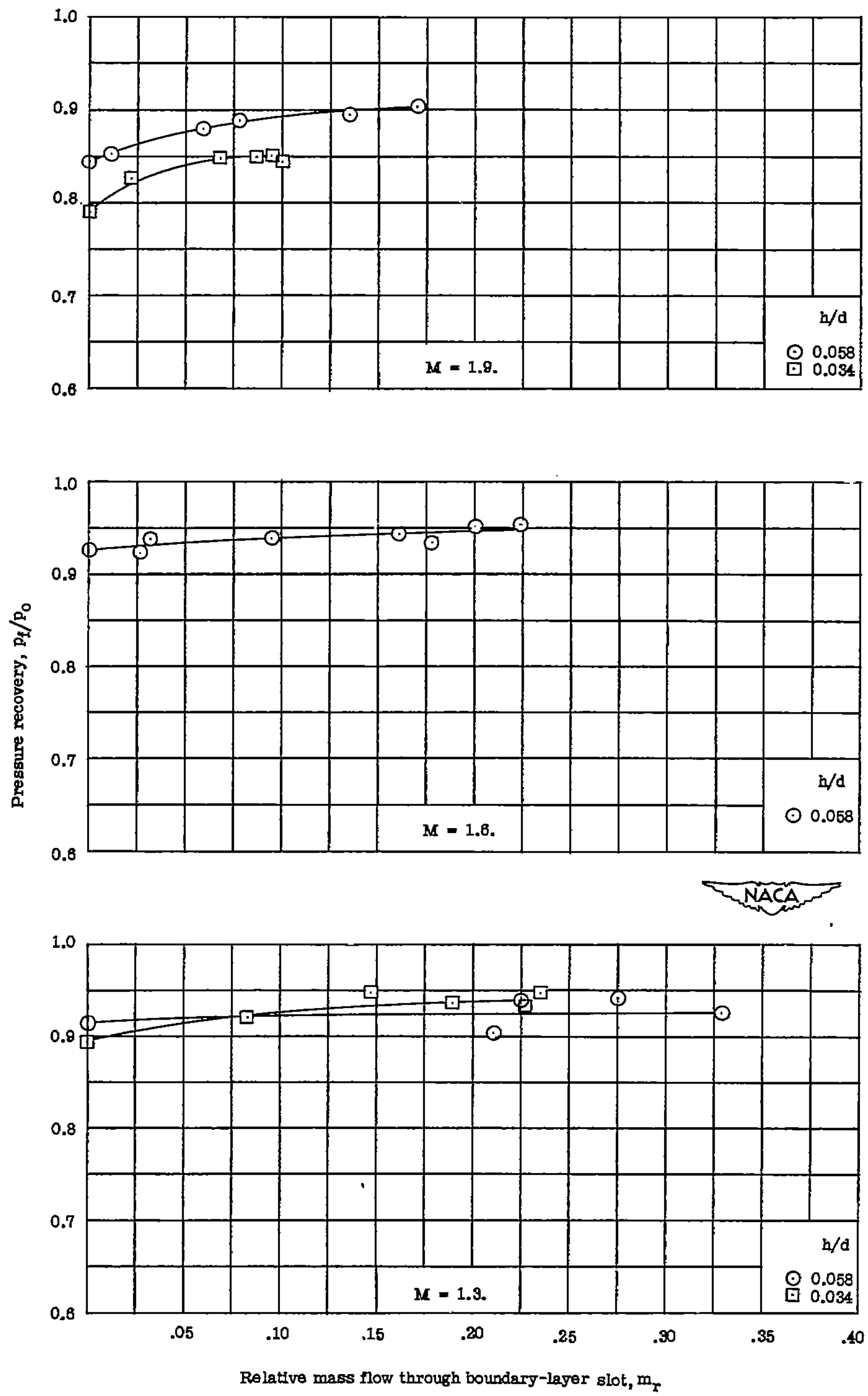

(a) 25° half-cone scoop inlet.

Figure 7.- Pressure recovery as a function of the relative mass flow through the boundary-layer slot for minimum m/m_o.

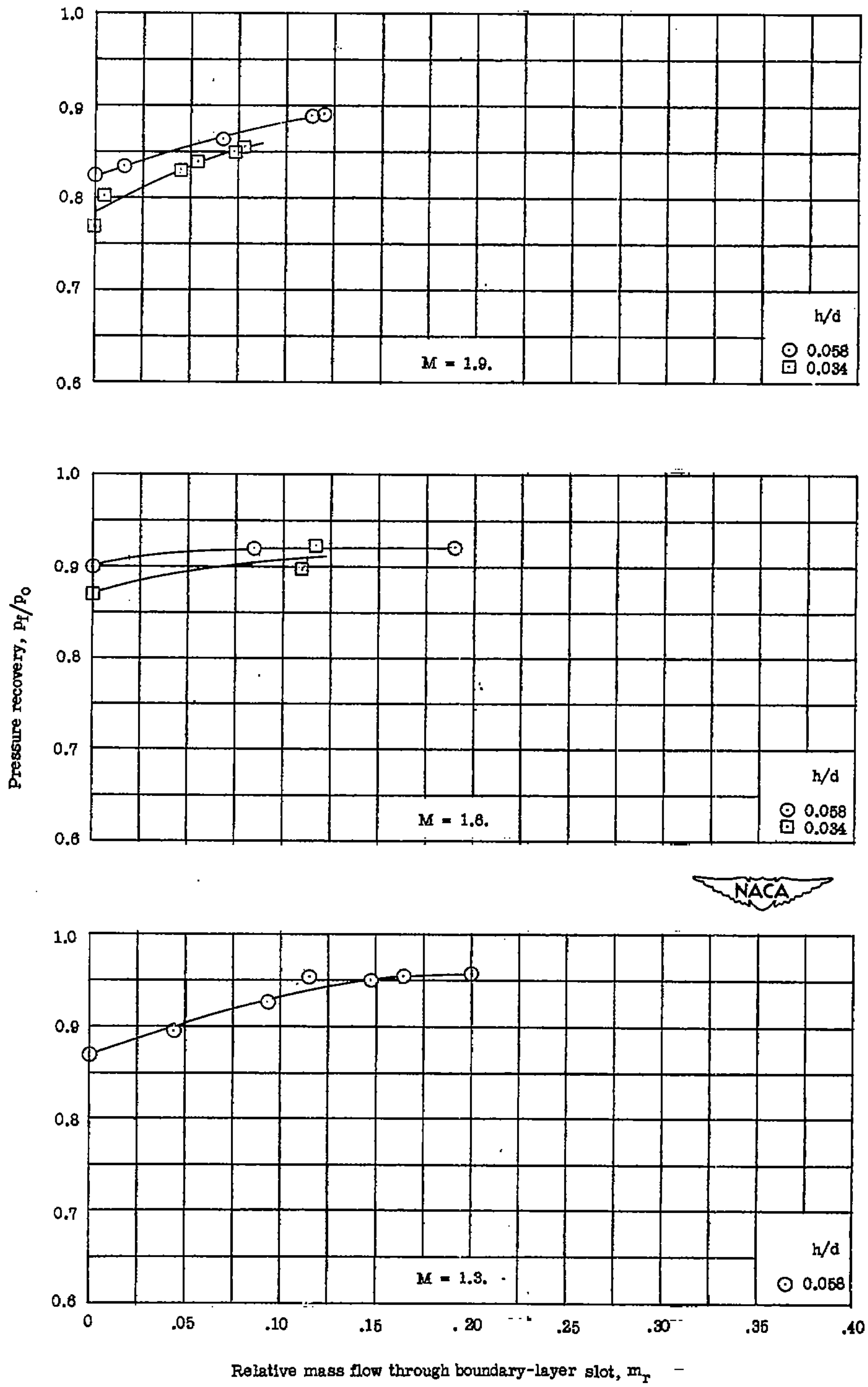

(b) 30° half-cone scoop inlet.

Figure 7.- Concluded.

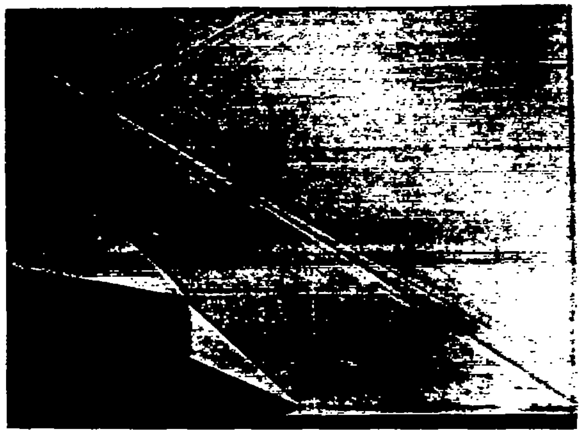

(a) M = 1.9.

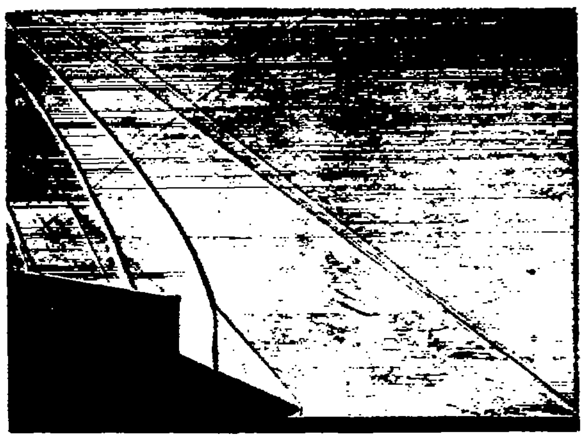

(b) M = 1.6.

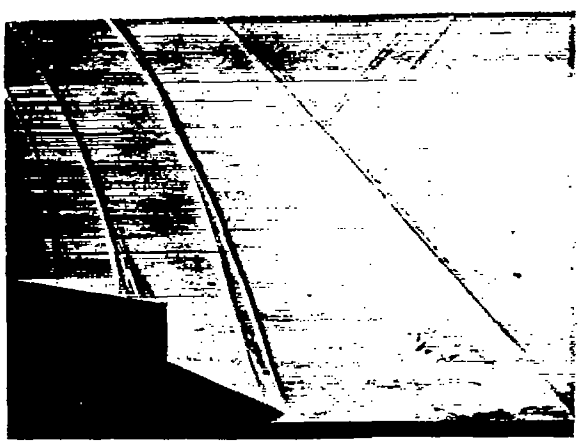

(c) M = 1.3.

L-70773

Figure 8.- Shadowgraph pictures of the 25° half-cone inlet for maximum m_r and minimum m/m_o at $\frac{h}{d} = 0.058$.

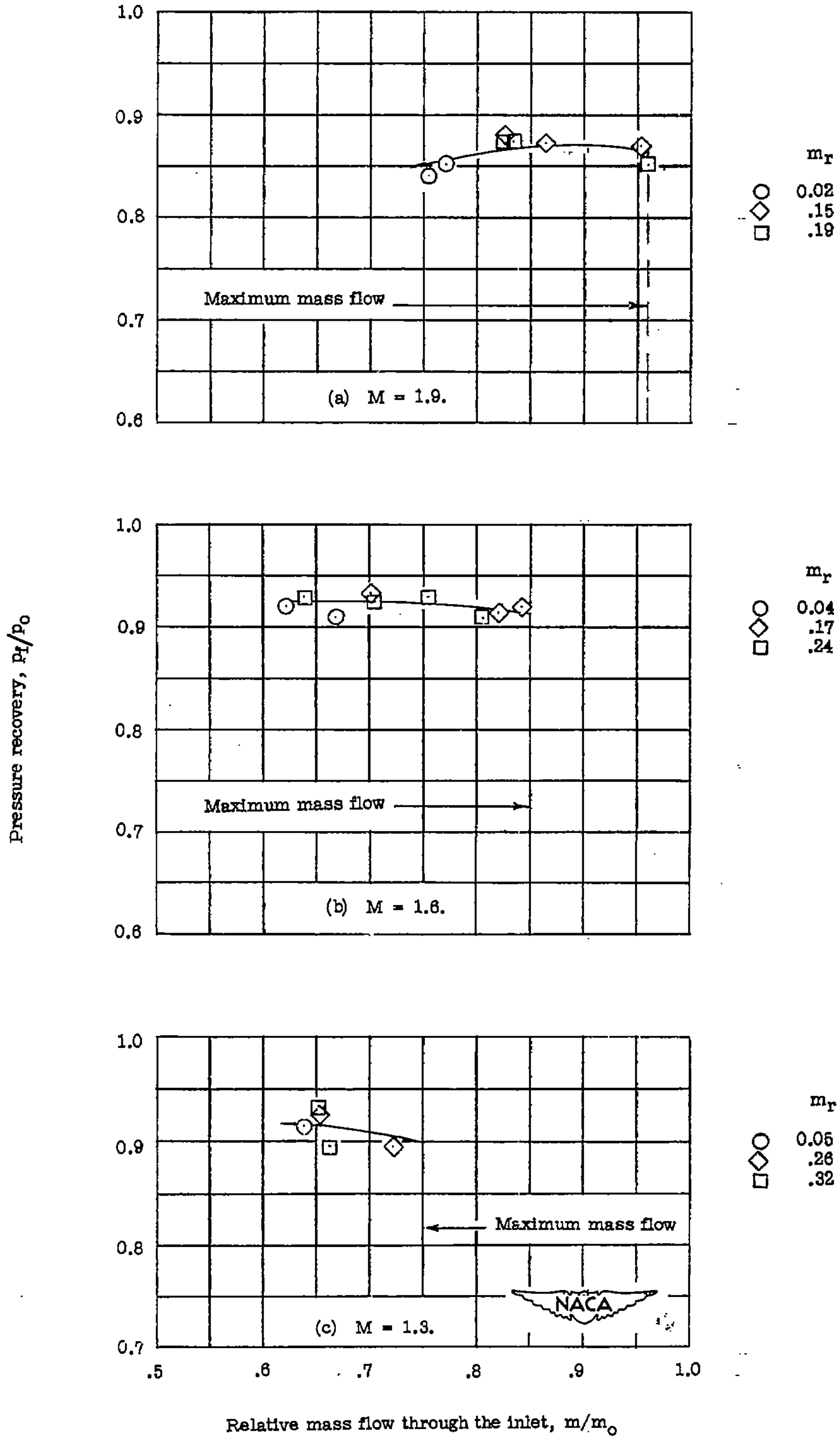

Figure 9.- Pressure recovery as a function of the relative mass flow through the 25° half-cone scoop inlet for $\frac{h}{d} = 0.058$.

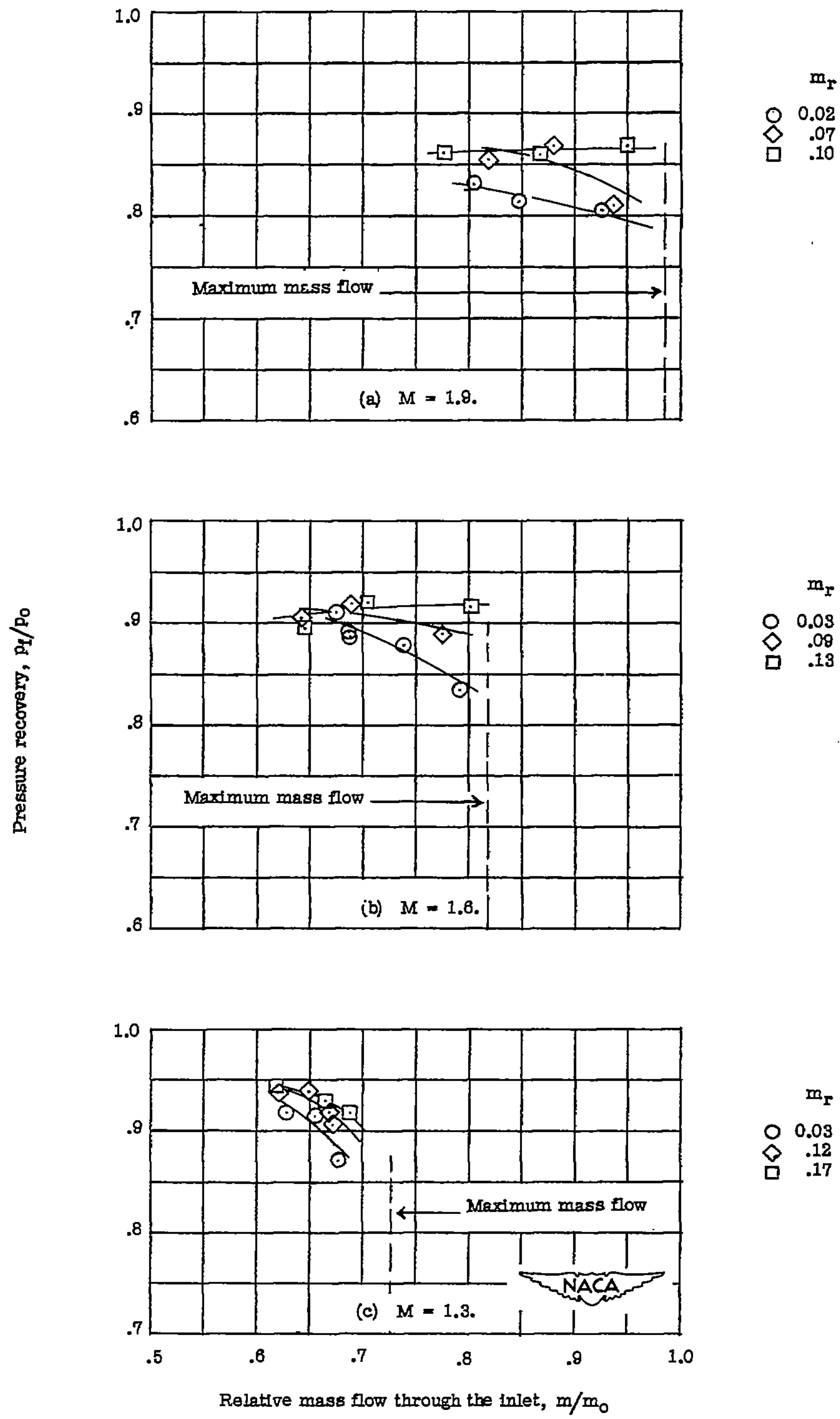

Figure 10.- Pressure recovery as a function of the relative mass flow through the 25° half-cone scoop inlet for $\frac{h}{d} = 0.034$.

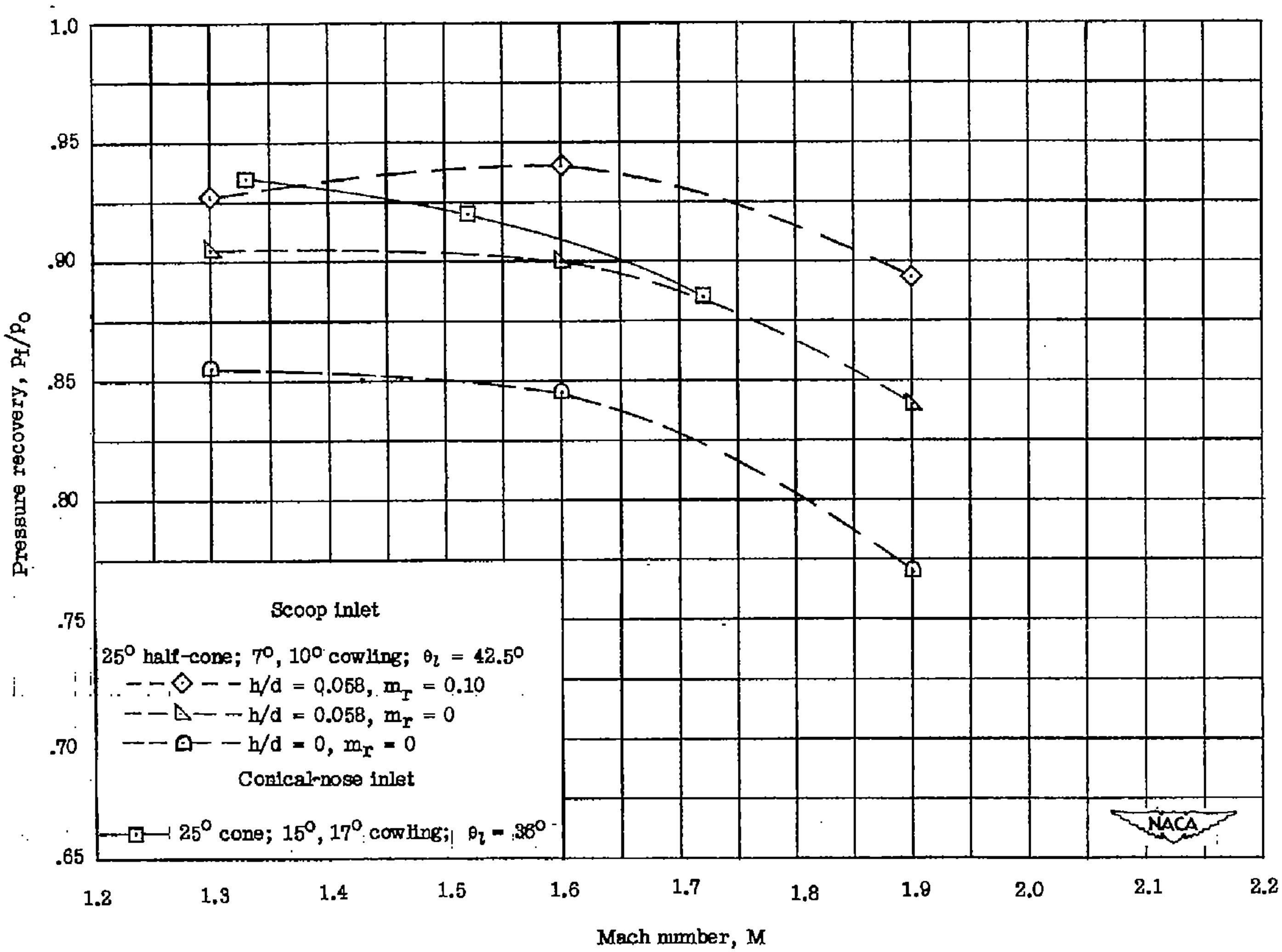

(a) 25° half-cone scoop inlet.

Figure 11.- Pressure recovery as a function of Mach number.

[redacted]

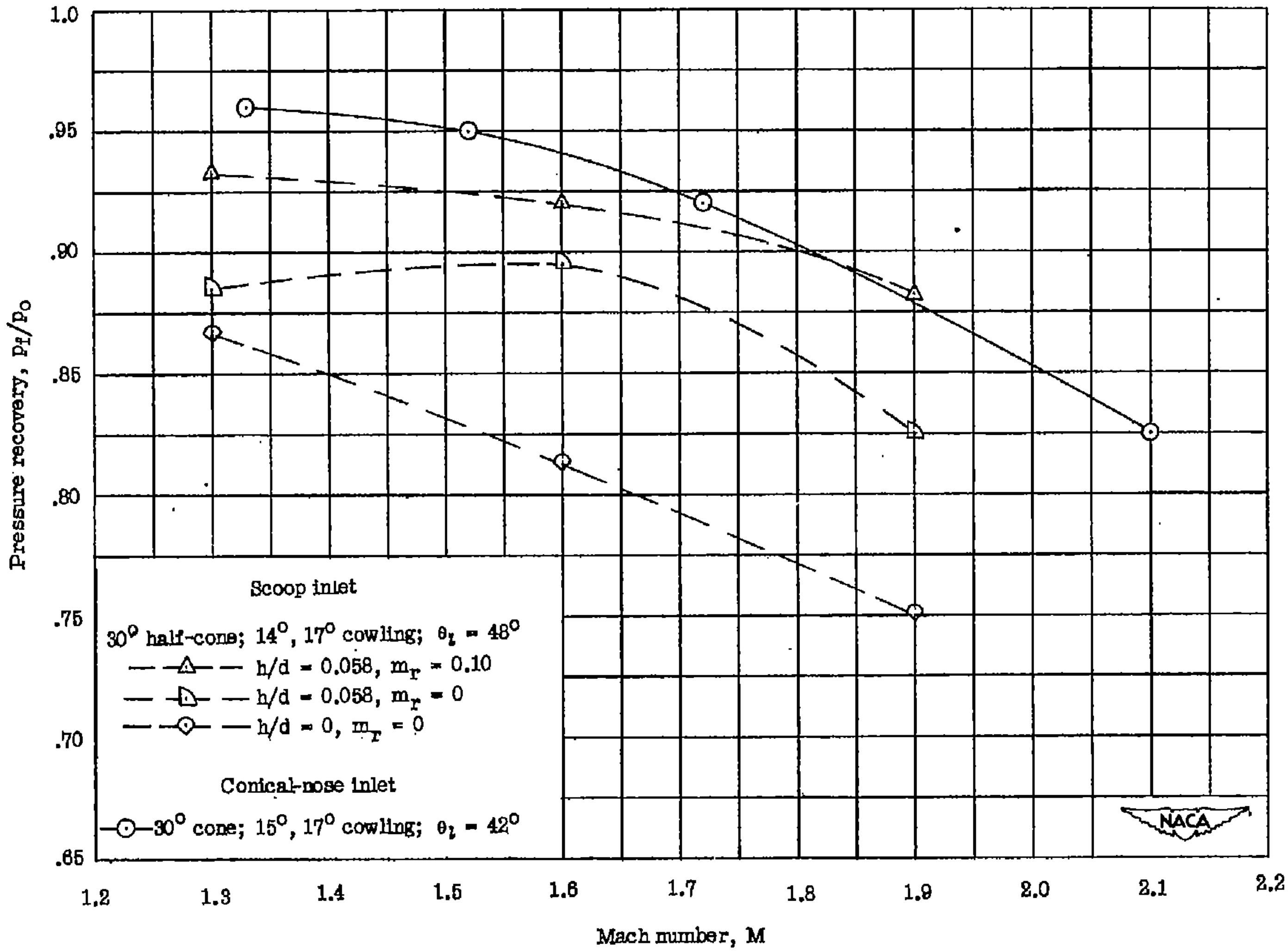

(b) 30° half-cone scoop inlet.

Figure 11.- Concluded.

[redacted]

NACA-Langley - 9-11-51 - 325